Journal of Marine Science and Technology

Volume 32 | Issue 3 Article 2

Evalution of the ability to infer tilt angle and size distributions of fish using a broadband scientific echosounder based on simulation

Jing Liu
Zhejiang Ocean University, No.1, Haida South Road, Lincheng Street, Dinghai District, Zhoushan City, Zhejiang Province, 316022, China, ljacoustic@163.com

Recommended Citation
Liu, Jing (2024) "Evalution of the ability to infer tilt angle and size distributions of fish using a broadband scientific echosounder based on simulation," *Journal of Marine Science and Technology*: Vol. 32: Iss. 3, Article 2.
DOI: 10.51400/2709-6998.2743
Available at: https://jmstt.ntou.edu.tw/journal/vol32/iss3/2

RESEARCH ARTICLE

Evaluation of the Ability to Infer Tilt Angle and Size Distributions of Fish Using a Broadband Scientific Echosounder Based on Simulation

Jing Liu

Zhejiang Ocean University, No.1, Haida South Road, Lincheng Street, Dinghai District, Zhoushan City, Zhejiang Province, 316022, China

Abstract

The biological information, such as species, size, and tilt angle, is crucial for converting the echo data into biomass information in acoustic surveys. Typically, the information can be obtained through trawl net sampling or underwater camera observations. However, both methods have some limitations. To overcome these limitations, scientists have utilized inversion methods with multi-frequency and broadband echosounders to derive biological information about fish, plankton, and krill. However, evaluating the reliability and accuracy of these inversion methods has been challenging due to the difficulty in obtaining accurate biological information. In this study, a numerical simulation method was used to generate fish school echoes with custom biological parameters, which were then used to infer biological information. The results showed that a reasonable distribution of fish tilt angles could be obtained through inversion using the mean target strength (TS) spectra. However, the cost function did not converge when the mean relative frequency response of volume backscattering (S_v) spectra was used. Furthermore, the error in inferring fish size using the mean TS spectra (assuming a broadband echosounder) was lower (5.7%) compared to the utilization of the mean TS at 120 kHz (assuming a traditional narrowband echosounder) with a higher error rate of 8.6%. This study particularly highlights the advantages of using broadband echosounders and the measured mean TS spectra for inferring biological information.

Keywords: Inversion, Target strength, Volume backscattering strength, Spectra

1. Introduction

Echosounders can transmit pulses of sound underwater and then receive the echoes that are reflected or scattered from underwater targets such as fish, plankton, and the seafloor. These echoes are used to gather information about the distribution of objects underwater [1]. As the focus on sustainable marine fishery resources grows, there is an increasing urgency to survey and assess fish stocks. Acoustic methods, including the use of echosounders, are being increasingly used in this field [2–6]. These fish stock surveys, conducted using scientific echosounders, are known as acoustic surveys. Acoustic surveys have several advantages compared to traditional methods such as using trawl nets and mathematical models based on catch data. Firstly, acoustic surveys provide high spatial and temporal resolution information, which allows for real-time acquisition of biological information in different layers of water. Secondly, they can quickly sample a large volume of water, making them highly efficient [7]. Lastly, acoustic surveys are non-invasive and do not harm the organisms being surveyed [1,8,9].

The echo integration method is used to calculate the cumulative backscattering cross section of underwater scatters observed by a scientific echosounder. The fish abundance can then be estimated by assuming that the echo energy received by an echosounder is proportional to the number of fish that are being insonified [1,10,11]. In acoustic surveys, multiple

Received 1 March 2024; revised 13 May 2024; accepted 14 May 2024.
Available online 9 September 2024
E-mail address: ljacoustic@163.com.

https://doi.org/10.51400/2709-6998.2743

species of underwater organisms are often present, making it necessary to assign the echo integration value proportionally to each organism. Therefore, information on the species composition of the organisms is required. Additionally, when converting the echo integration values to abundance, the mean target strength (TS) is used. The biomass can be calculated from the echo integration values by dividing them by the mean TS in linear form [10], further highlighting the mean TS as a crucial parameter in acoustic survey. The TS of fish is influenced by factors such as the species of the organism, anatomical characteristics (especially the presence or absence of swim bladder), body length, and tilt angle. Thus, biological information is essential for deciding the mean TS for fish [12]. Generally, the mean TS of fish can be determined using three methods. Firstly, there is *in situ* measurement, which is conducted in field water, and the targets can swim freely, however, the size distribution is unclear. Secondly, for *ex situ* measurement, the specimens are generally held in net cages or tethered by fishing line, then the TS values at different sizes and tilt angles are measured and finally the mean TS value was obtained combining the size and tilt angle distributions information. Thirdly, in theoretical modeling methods, similarly to the *ex situ* method, the TS values of the target at different sizes and tilt angles are calculated and averaged to obtain the mean TS. However, for the *ex situ* and theoretical modeling methods, the tilt angle distribution of the target is unclear. These descriptions highlight the crucial role of biological information like species composition, size, and tilt angle distributions in determining the mean TS of fish.

Various methods such as trawl sampling or underwater cameras have been frequently used to obtain biological information [13−16]. However, these methods have limitations. For example, trawl sampling will cause avoidance behavior of organisms, leading to biased sampling results, and it is also displays selectivity in its captures; The observation range of the underwater camera is affected by the turbidity of the water, and the effective observation distance is usually relatively short. To overcome these difficulties, the ideal solution will be to directly analyze the acoustic echoes to infer biological information without relying on additional equipment like trawls and cameras. In recent years, there have been many studies focusing on obtaining biological information from these echoes.

If the animal echoes characteristics such as TS or volume backscattering strength (S_v) at different frequencies exhibit dependencies on species, size, and tilt angle, it might be feasible to deduce biological details such as species, size, and tilt angle information from the echoes [1,17]. This will improve the accuracy of the mean TS measurement of fish. In previous studies, inversion methods based on multi-frequency technology have been frequently utilized to estimate the size distribution, tilt angle distribution, and density of organisms [18−23]. Additionally, attempts have been made to apply inversion methods based on broadband echosounder echo data to extract biological information [17,24,25]. Inversion methods based on broadband echosounders are believed to offer higher accuracy compared to traditional methods relying on narrowband echosounders. This occurs because broadband echosounders transmit pulses with continuous spectral information and enhance range resolution through pulse compression processing. This significantly boosts the information content in the echoes [26−28].

While the inversion method has many advantages, its accuracy is influenced by many factors such as how well the scattering model aligns with the biological scattering characteristics, the chosen inversion algorithm, the acoustic frequencies used. Additionally, accurate biological sampling using methods like trawls or underwater cameras can be challenging, making it difficult to assess the accuracy of the inversion methods employed. To address the above issues, it is optional to evaluate the accuracy of the inversion method with numerical simulations. This is because by using numerical simulation, arbitrary echoes with specific parameters (e.g., transducer settings, size distribution and tilt angle distribution) can be generated accurately according to the demand, thereby reduces the number of ambiguous parameters among the inversion algorithms. While studies have explored the utilization of multi-frequency acoustic data in inversion methods via numerical simulations (Chu et al., 2016a), no research has specifically assessed the accuracy of biological information inversion methods using broadband echosounder through numerical simulations.

This study aimed to investigate the ability of inferring fish size and tilt angle information from broadband echosounder echoes. Echoes from a large fish school were simulated, and the mean S_v and TS spectra were measured and used for the inversions of fish size and tilt angle distributions.

2. Materials and methods

2.1. Simulation of large fish school echoes

To simulate the echoes from a large school of fish, the following approach was employed. Initially, a broadband echosounder system was simulated, providing the necessary foundation for subsequent

calculations. Subsequently, the echoes from individual fish within the school were computed and simulated. Finally, the echoes from the entire school were generated by summing up all the individual echoes. Throughout this study, all the calculations and simulations were performed using Matlab (R2021b).

2.1.1. Single fish echo simulation

The broadband echosounder system and individual fish echoes were simulated based on the research conducted by Amakasu (2014). In this study, a commercial broadband echosounder EK80 (Kongsberg Maritime, Horten, Norway) with a split-beam broadband transducer (ES120-7C) was simulated. A circular piston transducer with radius of 5.642 was simulated to transmit the sound pulse and receive the echoes. Linear frequency modulated signal, $p_t(t)$ (frequency swept range from 90 to 170 kHz), with fast ramping and pulse duration of 2.048 ms was simulated, and the sampling rate was set at 500 kHz to avoid aliasing.

The $p_t(t)$ propagated to the target (fish) was referred to as incident pressure waveform, $p_i(t)$. The $p_i(t)$ is under the influence of the beam pattern of the transducer, $D(f)$, and the transmission loss, $L(f)$ [29,30]. For computational purposes, the frequency-domain forms of $D(f)$ and $L(f)$ were processed by the inverse Fourier transform. This allowed the transformation of these frequency-domain forms into their corresponding time-domain expressions, denoted as $d(t)$ and $l(t)$ [31].

$$D(f) = \frac{2J_1(ka\sin\theta)}{ka\sin\theta} \tag{1}$$

where f is the acoustic frequency, J_1 is the first kind of Bessel function with order 1, k is the wave number, a is the radius of the circular piston source, and θ is the off-axis angle of a target from the beam axis.

$$L(f) = r^{-1}e^{ikr}10^{-0.05\alpha(f)r} \tag{2}$$

where i is the imaginary unit, r is the range from transducer to targets, and α is the absorption coefficient.

$$p_i(t) = \left[p_t(t) * d(t)\right] * l(t) \tag{3}$$

where "*" is the convolution.

$p_i(t)$ interacts with the target and produces a scattered pulse $p_s(t)$. $p_s(t)$ is the result of convolution between $p_i(t)$ and the backscattering impulse response $f_{bs}(t)$ of a target. $f_{bs}(t)$ is obtained by performing an inverse Fourier transform on the backscattering amplitude $F_{bs}(f)$ of a target. The $F_{bs}(f)$ of the target (in this case, a fish) was calculated based on the modal-series-based prolate spheroid model (PSM) [32], one of the simplest and most exact models for a swimbladder [33]. The PSM was hereby adoped because the scattering ability of fish with swimbladders to sound mainly comes from the swimbladder [34].

Ultimately, under the influence of the beam pattern of the transducer and the transmission loss, the $p_i(t)$ propagated and was received by the transducer. The received echo, $p_r(t)$, could be expressed as:

$$p_r(t) = \left[p_s(t) * l(t)\right] * d(t) \tag{4}$$

2.1.2. School echo generation

A large fish school (7 m in height, 10 m in length, and 10 m in width) with a density (n) of 8 ind/m^3 and a volume much larger than that of the transducer beam was simulated as shown in Fig. 1. Each individual fish's position (x, y, z) within the school was randomly generated, assuming a random and uniform distribution. The transducer's coordinates were set at (0, 0, 0). All the individual fish in the school were assumed to have swimbladders, and the body length and tilt angle of the targets were assumed to follow truncated normal distributions. Additionally, the normal distribution in this study was defined by mean and standard deviation, N(mean, standard deviation). The distribution of body length was set to N(7 cm, 2 cm), with the maximum and minimum body lengths set at 11 and 3 cm respectively. The distribution of tilt angle was set to N(5 °, 10 °), with the maximum and minimum tilt angle range set at 35 and -25°. In this study, the tilt angle of the fish with its head up was considered positive, and the tilt angle with its head down was considered negative.

For the sake of convenience in implementing the model, the fish school was assumed swam along the x-axis, this means the body axis of each single fish was parallel to the x-z plane, as shown in Fig. 2. The off-axis angle in Equation (1) was calculated using the coordinate of the transducer (0, 0, 0) and the coordinate of the single target (x, y, z). The angle between the swimbladder axis and the pulse incident direction (θ_i in Fig. 2) was a key parameter in PSM, which could be calculated using vectors $\vec{a}$ ($-\cos\theta_t$, 0, $-\sin\theta_t$) and $\vec{b}$ (-x, -y, -z) in Fig. 2. The unit vector of $\vec{a}$ was derived from the tilt angle (θ_t) of the single target, while the unit vector of $\vec{b}$ was derived from the coordinates of the transducer (0, 0, 0) and the coordinate of the single target (x, y, z).

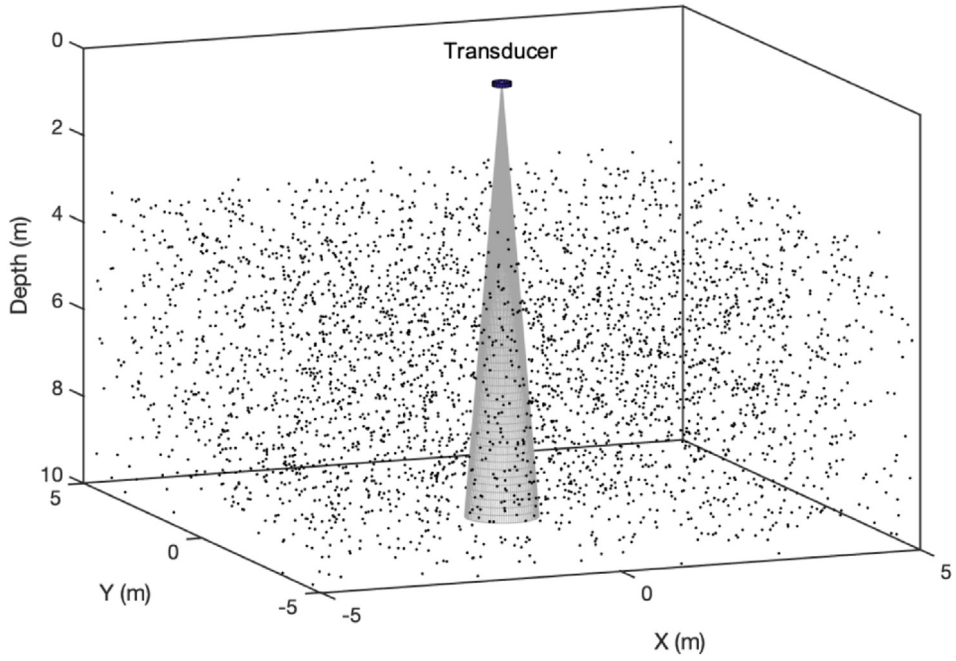

Fig. 1. Simulation of a large fish school (7 m in height, 10 m in length, and 10 m in width), with each black dot representing the location of each single fish.

To simulate each ping of echo data, the position coordinates, length, and tilt angle of each single target in the school were firstly simulated. The echo of each single target was simulated according to the method described above. Then, the echo of the entire school was obtained by coherently summing all the single target echoes [31,35]. Finally, the raw data of the simulated school echo was cross correlating with the transmit signal (used as replica signal) and the pulse-compressed echo of the school was obtained [27,35]. A total of 10 pings of the pulse-compressed school echoes were simulated in this study.

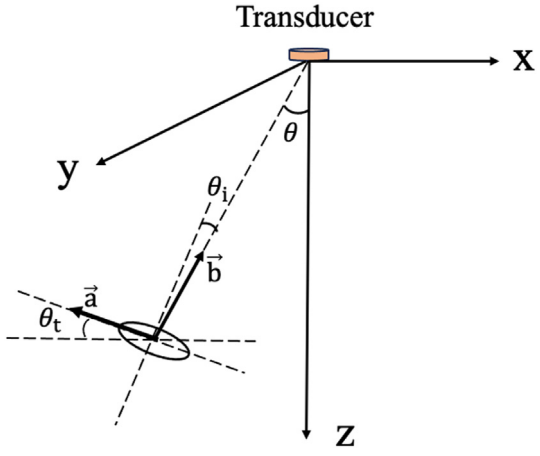

Fig. 2. Diagram of the coordinate system with the transducer as the origin position and the relative position to a single fish.

2.1.3. Volume backscattering strength and target strength spectra measurement

To ensure accurate S_v spectra measurement [hereinafter, the measured S_v spectra was noteed as $S_v(f)$], the calculations of $S_v(f)$ were performed iteratively and then averaged. The sampling window for the $S_v(f)$ calculations started at 5 m from the transducer surface and had a range of 1 m. The starting position of the sampling window was moved down by 0.1 m for each subsequent calculation, resulting in a total of 40 sampling windows between 5 and 10 m. The $S_v(f)$ were averaged over a total of 10 pings, resulting in a final mean S_v spectrum $\overline{S_v(f)}$ derived from 400 calculations.

The pulse-compressed echo data from each sampling window were extracted and adopted for $S_v(f)$ calculation. The $S_v(f)$ could be calculated by the following Equation [27,36]:

$$S_v(f) = 20\log_{10}\left(\frac{|CP_r(f)|}{|CP_t(f)|}\right) + 20\log_{10} r + 2\alpha r - 10\log_{10}(w) - \psi(f) \quad (5)$$

where $CP_r(f)$ is the fast Fourier transform of pulse-compressed fish school echo data within each sampling window, $CP_t(f)$ is the fast Fourier

transform of the pulse-compressed replica signal, r is the range from the transducer surface to the center of sampling window, w is the distance of the sampling window (1 m in this study), and $\psi(f)$ is the equivalent beam angle, calculated as $5.78/(ka)^2$, with k representing the wave number and a is the radius of the transducer [37].

Since the density of the fish school is known, according to the relationship between S_v and TS [1]: $S_v = nT_s$, it should be noted that the S_v and T_s are the linear formats of S_v and TS, the mean measured TS spectra [hereinafter, the measured TS spectra was noted as $TS(f)$] could hereby be derived from the mean S_v spectra as follows:

$$\overline{TS(f)} = \overline{S_v(f)} - 10\log_{10} n \tag{6}$$

2.2. Inference of orientation angle distribution

Given that the difference of mean S_v among frequencies could be used to infer biological information acoustically [38], the relative frequency response, $\Delta S_v(f)$, of the school was hereby normalized by the S_v value at 120 kHz, which was described as $\Delta S_v(f) = \overline{S_v(f)} - \overline{S_v(120\,\text{kHz})}$ [38]. Then,$\Delta S_v(f)$ was selected for inferring the tilt angle distribution of the fish in the simulated school.

The mean predicted TS spectra from PSM at a series of different tilt angle distributions were also calculated and used for the tilt angle distribution inversions by comparing with the $\Delta S_v(f)$ [hereinafter, the predicted mean TS spectra obtained directly from PSM were note as $\overline{TS_p(f)}$, averaged over the tilt angle and body length distributions] [32,39,40]. Specifically, the mean of tilt angle distribution was set from 0 to 30° in 1-degree increments, and the standard deviation of tilt angle distribution was set from 1 to 30° in 1-degree increments. The distribution of body lengths was assumed to be known through biological sampling. Therefore, the same mean and standard deviation of the body length distribution in the fish school echo simulation were used. The normalized TS spectra obtained from the prediction were expressed as $\Delta TS_p(f) = \overline{TS_p(f)} - \overline{TS_p(120\,\text{kHz})}$.

According to Equation (6), the shape of normalized TS spectra should ideally be the same as that of the normalized S_v spectra [41]. Consequently, the mean absolute error (ε) between $\Delta S_v(f)$ and $\Delta TS_p(f)$ was calculated for each pair of mean and standard deviation of tilt angle distributions and employed as a cost function to infer the optimal tilt angle distribution of the fish in the simulated school [42]. The pair of mean and standard deviation that resulted in the minimum ε were considered the optimal solutions obtained through the inversion algorithm. The ε is described as follows:

$$\varepsilon = \frac{1}{m}\sum_{i=1}^{m}\left|\Delta S_v(f_i) - \Delta TS_p(f_i)\right| \tag{7}$$

where $\Delta S_v(f_i)$ and $\Delta TS_p(f_i)$ are the normalized spectra of $\overline{S_v(f)}$ and $\overline{TS_p(f)}$ at the ith frequency, and m is the total number of frequencies.

Since the range resolution of broadband echosounder is higher than traditional narrowband echosounder, it is hopeful to obtain enough single target echoes during acoustic survey. And it is also possible to infer the tilt angle distribution with the TS spectra instead of the normalized TS spectra. Therefore, the tilt angle distribution inversion using the $\overline{TS(f)}$ and $\overline{TS_p(f)}$ was also performed and investigated. Similarly, the mean absolute error (ε) between $\overline{TS(f_i)}$ and $\overline{TS_p(f_i)}$ was calculated for each pair of mean and standard deviation of tilt angle distributions and used as a cost function to infer the optimal tilt angle distribution of the fish in the simulated school [42]. The pair of mean and standard deviation that resulted in the minimum ε were considered the optimal solutions obtained through the inversion algorithm. The ε is described as follows:

$$\varepsilon = \frac{1}{m}\sum_{i=1}^{m}\left|\overline{TS(f_i)} - \overline{TS_p(f_i)}\right| \tag{8}$$

where $\overline{TS(f_i)}$ and $\overline{TS_p(f_i)}$ are the mean measured TS and the mean predicted TS at the ith frequency, and m is the total number of frequencies.

2.3. Inference of fish size distribution

Assume the tilt angle distribution of the fish in the simulated school is known, then the body length distribution of the fish could be inferred from the $\overline{TS(f)}$ and the $\overline{TS_p(f)}$. Hence, to maintain consistency with the real values in the simulation, the mean and standard deviation of the tilt angle distribution used in the inversion were set at 5 and 10° respectively. The mean body length was set from 4 to 10 cm in 0.1-cm increments for inversion. For each mean body length, the predicted TS spectra under the above-mentioned tilt angle distributions were calculated with PSM and averaged to get the $\overline{TS_p(f)}$.

To investigate the difference in accuracy of body length inversion between narrowband and broadband echosounders, two inversion methods were employed. For the first method, the measured TS at

a single-specific frequency (120 kHz) was compared with the predicted TS (120 kHz) during the inversion, and the corresponding mean absolute error ε_s was used as cost function:

$$\varepsilon_s = \overline{TS(120\,\mathrm{kHz})} - \overline{TS_p(120\,\mathrm{kHz})} \quad (9)$$

where $\overline{TS(120\,\mathrm{kHz})}$ is the measured mean TS of the simulated fish school at 120 kHz, and $\overline{TS_p(120\,\mathrm{kHz})}$ is the predicted mean TS at 120 kHz.

For the second method, the mean absolute error among frequencies of the $\overline{TS(f)}$ and the $\overline{TS_p(f)}$ was calculated following Equation (8) to simulate the inversion with broadband echosounder.

3. Results

3.1. Measured volume backscattering strength spectra

Fig. 3 presents the results of analyzing 400 S_v spectra obtained from the simulated school echo. It was observed that while individual S_v spectra appeared to fluctuate, the averaged S_v spectrum became relatively stable. The shape of the near-flat mean S_v spectrum closely resembled that of the TS spectra of typical fishes with swimbladder, as described in previous studies [27,43]. Additionally, the mean measured TS spectrum in the simulated fish school was calculated following Equation (6), and the results are shown in Fig. 4. For comparison, the mean TS spectrum calculated by PSM is also presented in Fig. 4. As shown in the figure, the measured TS spectrum and the predicted TS spectrum by PSM exhibited a good agreement. The mean and standard deviations of the measured and predicted TS spectra were −47.18 dB and 0.32 dB, respectively, and −47.35 dB and 0.09 dB, respectively. Besides, the mean absolute error between the measured and predicted TS spectra was 0.26 dB. This provides further evidence that the simulation process for the fish school echoes and the methods used to calculate S_v and TS spectra are correct.

3.2. Inversion of tilt angle distribution

Fig. 5 shows the results of tilt angle distribution inference. As shown in Fig. 5(a), the ε never exceeded 1 dB, in most cases the variation of ε was small and less than 0.3 dB, and there was no extreme minima of ε when using $\Delta S_v(f_i)$ and $\Delta TS_p(f_i)$ for the inversion process. This also indicated that the trends of $\Delta S_v(f_i)$ and $\Delta TS_p(f_i)$ remained the same for different tilt angle distributions. Therefore, $\Delta S_v(f_i)$ and $\Delta TS_p(f_i)$ could not be used to infer the tilt angle distribution of the fish in the simulated school. However, Fig. 5(b) revealed that ε clearly converged to a specific region. Furthermore, the mean and standard deviation of the real tilt angle distribution $N(5\,^\circ, 10\,^\circ)$ used in the simulation fell within the convergence region. This indicated that the average TS spectra were more suitable for inferring the tilt angle

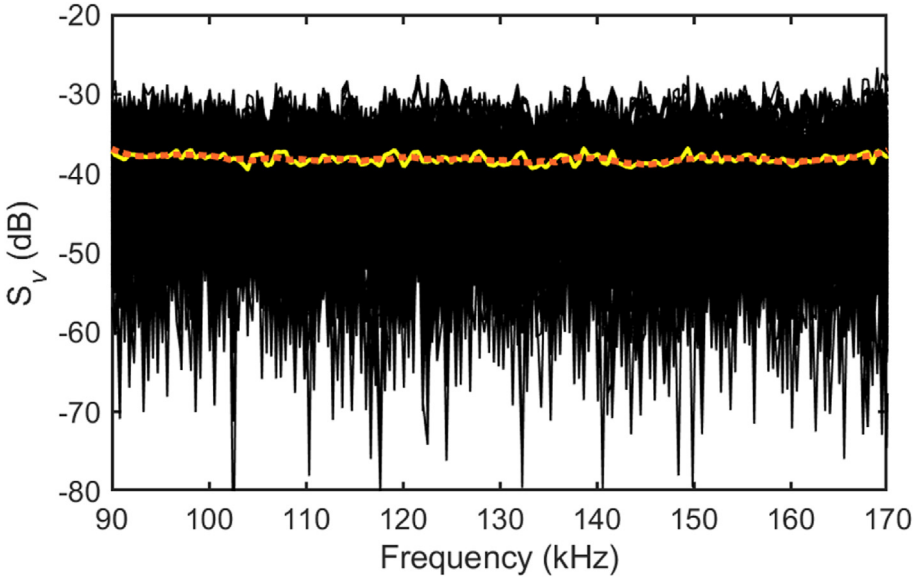

Fig. 3. Measured S_v spectra from the simulated fish school echoes. The black lines are the 400 measurements of S_v spectra, the yellow line is the averaged S_v spectrum derived from the 400 S_v spectra on a linear scale, and the red dot line is the result of the 10-points moving mean processing of the averaged S_v spectrum. The moving mean processing was carried out using Matlab, and the sliding window of "10-points" was determined through trial-and-error.

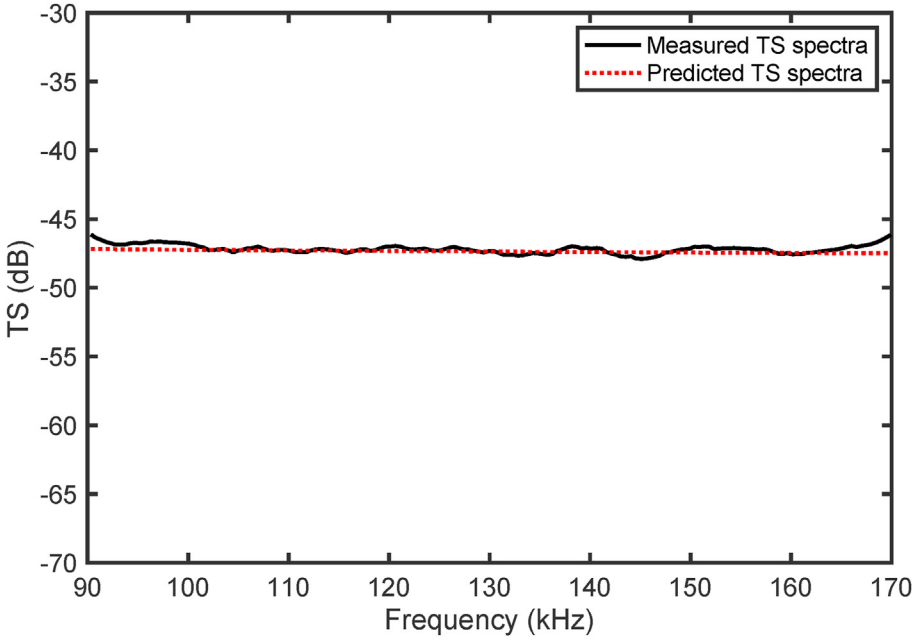

Fig. 4. Mean TS spectrum of the fish in the simulated fish school. The black line is the mean measured TS spectra from the simulated school, and the red dot line is the mean predicted TS spectra from PSM.

distribution of fish through the inversion method compared to the average S_v spectra. This occurred because not only the shapes of the spectra, but also their amplitudes were included in the tilt angle distribution inversion when using the averaged TS spectra $\overline{TS(f)}$ and $\overline{TS_p(f)}$. However, when $\Delta S_v(f_i)$ and $\Delta TS_p(f_i)$ were used for inversion, only the shapes of the spectra were involved.

3.3. Inversion of fish size

The results of fish size estimation are presented in Fig. 6. As shown in the figure, the inferred sizes using the two inversion methods (inversion with single frequency TS and TS spectra) discussed in Section 2.3 were 7.3 cm and 7.5 cm, respectively. The errors in body length obtained by these two inversion methods were 4.3% and 7.1% respectively, when compared to the actual body length of 7 cm. This suggested that biological information derived from inversion using TS spectra from a broadband echosounder surpassed that from a traditional narrowband echosounder. This was because the TS spectra contained more information and enhanced the accuracy of the inversion process.

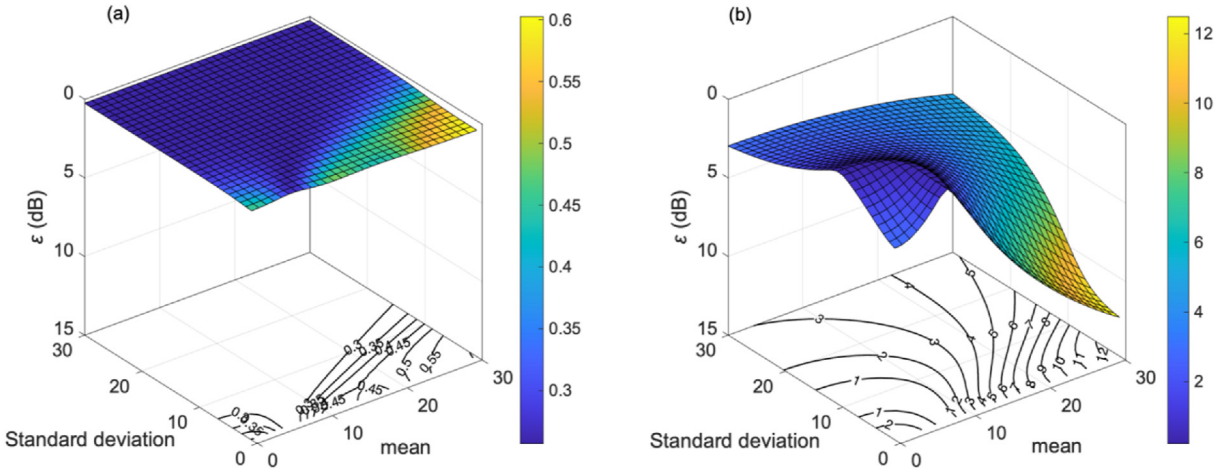

Fig. 5. Results of tilt angle distribution inference. The surface plot and contour plot represent the ε under different mean and standard deviations of the candidate tilt angle distributions. (a): the mean absolute error (ε) between $\Delta S_v(f)$ and $\Delta TS_p(f)$, and (b): the mean absolute error (ε) between $\overline{TS(f)}$ and $\overline{TS_p(f)}$.

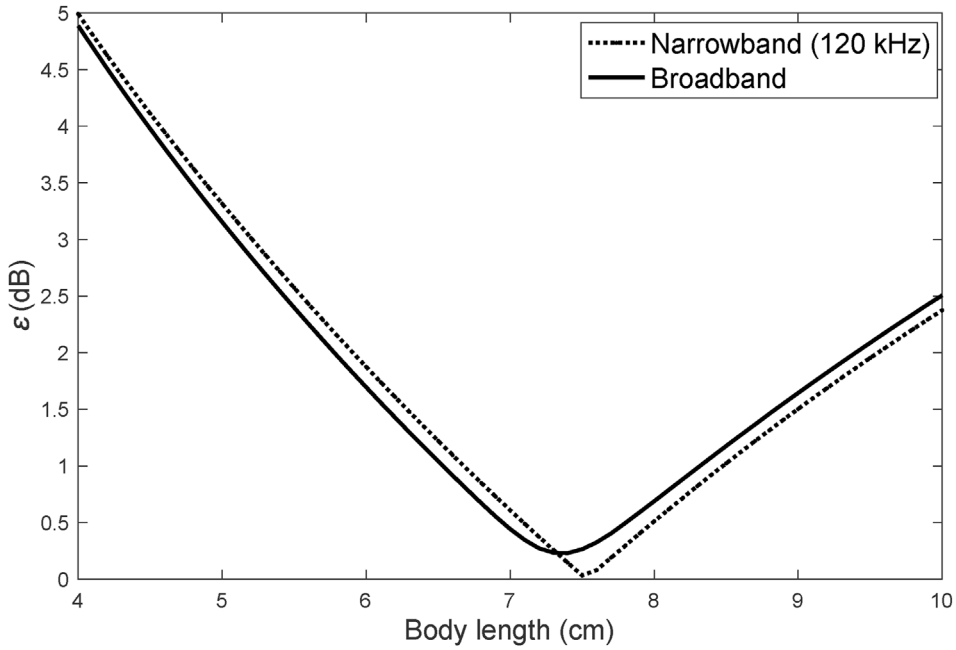

Fig. 6. Results of fish size inference.

4. Discussion

4.1. Accuracy of tilt angle distribution inference with inversion

Previous studies employed inversion methods to infer biological information on fish, plankton, and krill, utilizing multi-frequency and broadband echosounders. However, due to challenges in obtaining accurate biological sampling information, the accuracy of the inversion results was difficult to assess [17−20,22−25,39]. In this study, the numerical simulation method was employed to generate large fish school echoes with custom biological parameters, and some biological parameters of the fish were estimated using the inversion method. This study made the first attempt to quantitatively investigate the accuracy of the inversion method with broadband echosounder.

The mean TS spectrum of the fish in the simulated school was calculated and compared with the predicted mean TS spectrum, and the correctness of the simulated broadband echosounder system and the TS spectra calculation methods was verified. In addition, it was found that the S_v and TS spectra calculated from a large number of measurements were closer to the predicted spectra. This is consistent with the findings of Amakasu [31]. Therefore, when inferring biological information, it is important to consider the method and accuracy of S_v or TS spectra measurement to avoid significant errors in inversions caused by the inaccurate S_v or TS spectra measurement.

In the tilt angle distribution inference, it was found that the ε values obtained from the inversion of $\Delta\ S_v(f)$ and $\Delta TSp(f)$ did not converge to a specific coordinate or region, and all the ε values were less than 1 dB (see Fig. 5-a). This was attributed to the similar shape of the measured S_v spectra of the simulated fish at different tilt angle distributions in this frequency band. Therefore, when using $\Delta\ S_v(f)$ for inversion, the spanning frequency band of the used transducer should be particularly considered. For instance, reliability can be enhanced when the frequency band of the transducer used in inversion spans the transition from Rayleigh to geometric scattering of the targets. However, the S_v measurements of fish in the Rayleigh region generally require the transducers that can transmit pulse at a few hertz to a few kilohertz, which is not always feasible with commonly used commercial echosounders [20]. Considering the high range resolution of broadband echosounders, in this study, the $\overline{TS(f)}$ was also used for the inference of tilt angle distribution. Fig. 5-b unveiled that the ε values converged in an arc-shaped area rather than a specific point. To obtain the optimal inversion result, all the candidate mean and standard deviation values where ε was less than 0.5 dB were selected and averaged to obtain the final inversion result: N (4.5 °, 8.4 °). Thus, the errors in the mean and standard deviation obtained from the inversion method were 10% and 16%, respectively. Despite the

modest accuracy of inversion using $\overline{TS(f)}$, it was demonstrated to be more effective than $\Delta\ S_v(f)$ in inferring the tilt angle distribution with inversion methods. In previous studies, Jaffe and Roberts [44] used a broadband system and Sinc function (SNC) model to estimate the fish orientation in a laboratory, demonstrated the average error between 5.5° and 17°. Stanton et al. [24] analyzed the temporal characteristics of the echoes of individual fish in a laboratory, and concluded that the error of the inferred orientation from the pulse-compressed echoes would approximately range from 5% to 10% under ideal conditions. Therefore, the accuracy of the inferred orientation through the measured and predicted TS spectra in this study was comparable to that in other studies.

4.2. Fish size inference

The fish body length inferred from the mean TS spectra was 7.4 cm, while the body length inferred from the mean TS at 120 kHz was 7.6 cm. The errors in the body length estimation using these two methods were 5.7% and 8.6%, respectively. This indicated that the broadband echosounders are more advantageous for accurately determining the fish body length. While the inversion using a single frequency TS at 120 kHz (similar to a narrowband echosounder) could also provide results close to the actual body length (with an error of less than 10%), it should still be noted that the range resolution of traditional narrowband echosounders was limited by the pulse length, making it challenging to detect enough single-target echoes for inferring biological information.

Apart from the inversion method, there are other methods that have been employed to estimate fish body lengths. For instance, the high range resolution of broadband echosounders allows for the use of pulse-compressed echo waveforms to infer fish size [28,45]. Specifically, Kubilius et al. [28] analyzed the pulsed-compressed echoes of simulated fish made from polyvinyl alcohol cryogel. Their aim was to estimate the size, and ultimately, they demonstrated an error range of 5.5%−8.5% for targets longer than approximately 200 mm and thicker than about 20 mm. Besides, Kubilius et al. [45] analyzed the pulsed-compressed echoes of tethered fish ranging in standard length from 239 to 491 mm and confirmed a size inference error of 2.2%−3.9%. Additionally, analyzing the mean TS of targets in relation to the body length of targets can be a useful method for inferring fish size. For instance, Puig-Pons et al. estimated the body size of Bluefin Tuna in sea cages by establishing the relationship between TS and body size. They confirmed an error in size estimation of less than 5% [46]. Hence, the accuracy of estimating the body length of fish through their TS spectrum is comparable to other methods mentioned above.

While broadband echosounders hold great potential for inferring biological information, there are several considerations to be highlighted. Firstly, the precise measurement of TS and S_v spectra play a critical role in the accuracy of inversion results. Especially when conducting TS spectra measurement, care should be taken to avoid multi-target echoes, and the appropriate Fourier transform window should be considered [47]. Secondly, it is of considerable significance to choose a suitable theoretical model for inversion. The closeness between the scattering spectra derived from the theoretical model and the actual scattering spectra of the targets influences the accuracy of the inversion results. Thirdly, reasonable assumption conditions affect inversion outcomes. Lastly, differences in inversion algorithms can yield varying results [20,21]. In this study, the simplest inversion algorithm was utilized, which involved using the mean absolute error between the measured and predicted TS or S_v values as a cost function. The effects of different inversion algorithms on the inference of biological information should still be explored by employing numerical simulation methods in future studies.

5. Conclusions

In this research, the accuracy during biological information inference was investigated using numerical simulation. The results confirmed that using TS spectra yielded better results for estimating the tilt angle and size distributions of fish, further highlighting the significance of broadband echosounders and TS spectra in inferring biological information. In addition, it was hereby observed that the mean absolute error of mean and standard deviation in tilt angle inversion did not converge to a point, but rather to an area, making it necessarily important to carefully determine the optimal values for the mean and standard deviation of tilt angle based on convergence characteristics, rather than solely focusing on minimizing the cost function. Additionally, the present study demonstrated the convenience of using numerical simulation for evaluating biological information inference through inversion. Numerical simulation could also be used in the future to evaluate other studies such as acoustic species classification.

Ethics approval

Ethical approval was not applicable for the present study because this study did not involve human or live animal experiments.

Funding

This study was supported by Zhejiang ocean university's program of introduce talent research fund.

Conflict of interest

The author declares there are no competing interests.

References

[1] Simmonds J, MacLennan DN. Fisheries acoustics: theory and practice. John Wiley & Sons; 2008.
[2] Pickrill RA, Todd BJ. The multiple roles of acoustic mapping in integrated ocean management, Canadian Atlantic continental margin. Ocean Coast Manag 2003;46(6−7):601−14. https://doi.org/10.1016/S0964-5691(03)00037-1.
[3] Godøl OR, Handegard NO, Browman HI, Macaulay GJ, Kaartvedt S, Giske J, et al. Marine ecosystem acoustics (MEA): quantifying processes in the sea at the spatio-temporal scales on which they occur. ICES J Mar Sci 2014;71(8):2357−69. https://doi.org/10.1093/icesjms/fsu116.
[4] Klemas V. Fisheries applications of remote sensing: an overview. Fish Res 2013;148:124−36. https://doi.org/10.1016/j.fishres.2012.02.027.
[5] Aura CM, Nyamweya CS, Owili M, Gichuru N, Kundu R, Njiru JM, et al. Checking the pulse of the major commercial fisheries of lake Victoria Kenya, for sustainable management. Fish Manag Ecol 2020;27(4):314−24. https://doi.org/10.1111/fme.12414.
[6] Swart S, Zietsman JJ, Coetzee JC, Goslett DG, Hoek A, Needham D, et al. Ocean robotics in support of fisheries research and management. Afr J Mar Sci 2016;38(4):525−38. https://doi.org/10.2989/1814232X.2016.1251971.
[7] Minami K, Kita C, Shirakawa H, Kawauchi Y, Shao H, Tomiyasu M, et al. Acoustic characteristics of a potentially important macroalgae, Sargassum horneri, for coastal fisheries. Fish Res 2021;240:105955.
[8] Taylor JC, Ebert EF, Kracker LM. Mapping fish densities using fishery acoustics. Fish Benthic Commun Flower Garden Banks Nation Marine Sanct: Sci Supp Sanct Manage 2014;179:260.
[9] Chu D, Thomas R, Clemons J, Parker-Stetter S, Pohl J, Clemons J, et al. Application of acoustic technologies to study the temporal and spatial distributions of the Pacific hake (Merluccius productus) in the California Current System. J Acoust Soc Am 2016;139:2173.
[10] Foote KG. Fish target strengths for use in echo integrator surveys. J Acoust Soc Am 1987;82(3):981−7.
[11] Maclennan DN. Acoustical measurement of fish abundance. J Acoust Soc Am 1990;87(1):1−15.
[12] Foote KG. Importance of the swimbladder in acoustic scattering by fish: a comparison of gadoid and mackerel target strengths. J Acoust Soc Am 1980;67(6):2084−9. https://doi.org/10.1121/1.384452.
[13] Kotwicki S, Ressler PH, Ianelli JN, Punt AE, Horne JK. Combining data from bottom-trawl and acoustic-trawl surveys to estimate an index of abundance for semipelagic species. Can J Fish Aquat Sci 2018;75(1):60−71.
[14] Sawada K, Uchikawa K, Matsuura T, Sugisaki H, Amakasu K, Abe K. In situ and ex situ target strength measurement of mesopelagic lanternfish, Diaphus Theta (Family Myctophidae). J Mar Sci Technol 2011;19(3):10.
[15] Sawada K, Takahashi H, Abe K, Ichii T, Watanabe K, Takao Y. Target-strength, length, and tilt-angle measurements of Pacific saury (Cololabis saira) and Japanese anchovy (Engraulis japonicus) using an acoustic-optical system. ICES J Mar Sci 2009;66(6):1212−8.
[16] McQuinn IH, Simard Y, Stroud TWF, Beaulieu JL, Walsh SJ. An adaptive, integrated "acoustic-trawl" survey design for Atlantic cod (Gadus morhua) with estimation of the acoustic and trawl dead zones. ICES J Mar Sci 2005;62(1):93−106.
[17] Traykovski LVM, O'driscoll RL, Mcgehee DE. Effect of orientation on broadband acoustic scattering of Antarctic krill Euphausia superba: implications for inverting zooplankton spectral acoustic signatures for angle of orientation. J Acoust Soc Am 1998;104(4):2121−35.
[18] Chu D, Foote KG, Stanton TK. Further analysis of target strength measurements of Antarctic krill at 38 and 120 kHz: comparison with deformed cylinder model and inference of orientation distribution. J Acoust Soc Am 1993;93(5):2985−8.
[19] Korneliussen RJ, Heggelund Y, Eliassen IK, Øye OK, Knutsen T, Dalen J. Combining multibeam-sonar and multifrequency-echosounder data: examples of the analysis and imaging of large euphausiid schools. ICES J Mar Sci 2009;66(6):991−7.
[20] Horne JK, Jech JM. Multi-frequency estimates of fish abundance: constraints of rather high frequencies. ICES J Mar Sci 1999;56(2):184−99.
[21] Chu D, Lawson GL, Wiebe PH. Estimation of biological parameters of marine organisms using linear and nonlinear acoustic scattering model-based inversion methods. J Acoust Soc Am 2016;139:2885−95. https://doi.org/10.1121/1.4948759.
[22] Lawson GL, Wiebe PH, Ashjian CJ, Stanton TK. Euphausiid distribution along the Western Antarctic Peninsula-Part B: distribution of euphausiid aggregations and biomass, and associations with environmental features. Deep Sea Res 2008;2(55):432−54. https://doi.org/10.1016/j.dsr2.2007.11.014.
[23] Holliday DV, Donaghay PL, Greenlaw CF, Napp JM, Sullivan JM. High-frequency acoustics and bio-optics in ecosystems research. ICES J Mar Sci 2009;66(6):974−80.
[24] Stanton TK, Reeder DB, Jech JM. Inferring fish orientation from broadband-acoustic echoes. ICES J Mar Sci 2003;60(3):524−31.
[25] Amakasu K, Mukai T, Moteki M. Measurement of the volume-backscattering spectrum from an aggregation of Antarctic krill and inference of their length-frequency distribution. Polar Sci 2017;12:79−87. https://doi.org/10.1016/j.polar.2017.02.007.
[26] Andersen L, Ona E, Macaulay G. Measuring fish and zooplankton with a broadband split beam echo sounder. In: 2013 MTS/IEEE OCEANS-Bergen. vol. 2013. IEEE; 2013. p. 1−4.
[27] Stanton TK, Chu D, Jech JM, Irish JD. New broadband methods for resonance classification and high-resolution imagery of fish with swimbladders using a modified commercial broadband echosounder. ICES J Mar Sci 2010;67(2):365−78. https://doi.org/10.1093/icesjms/fsp262.
[28] Kubilius R, Macaulay GJ, Ona E. Remote sizing of fish-like targets using broadband acoustics. Fish Res 2020;228:105568. https://doi.org/10.1016/j.fishres.2020;105568.
[29] Francois RE, Garrison GR. Sound absorption based on ocean measurements. Part II: boric acid contribution and equation for total absorption. J Acoust Soc Am 1982;72(6):1879−90. https://doi.org/10.1121/1.388673.
[30] Medwin H, Clay CS. Fundamentals of acoustical oceanography. Elsevier; 1998.
[31] Amakasu K. Computer simulation of broadband single-target echo waveforms and its application. J Mar Acoust Soc Jpn 2014;41(4):183−90. https://doi.org/10.3135/jmasj.41.183.

[32] Furusawa M. Prolate spheroidal models for predicting general trends of fish target strength. J Mar Acoust Soc Jpn (E) 1988;9(1):13−24. https://doi.org/10.1250/ast.9.13.
[33] Sawada K, Matsuura T, Fukuda Y. Target strength of juvenile salmon, Oncorhynchus keta, for acoustic monitoring. J Mar Acoust Soc Jpn 2022;49(2):46−67.
[34] Foote KG. Importance of the swimbladder in acoustic scattering by fish: a comparison of gadoid and mackerel target strengths. J Acoust Soc Am 1980;67:2084−9.
[35] Lee WJ, Stanton TK. Statistics of broadband echoes: application to acoustic estimates of numerical density of fish. IEEE J Ocean Eng 2015;41(3):709−23. https://doi.org/10.1109/JOE.2015.2476619.
[36] Demer DA, Andersen LN, Bassett C, Berger L, Chu D, Condiotty J, et al. Evaluation of a wideband echosounder for fisheries and marine ecosystem science. ICES (Int Counc Explor Sea) Coop Res Rep 2017.
[37] Medwin H. Sounds in the sea: from ocean acoustics to acoustical oceanography. Cambridge University Press; 2005.
[38] Bassett C, De Robertis A, Wilson CD. Broadband echosounder measurements of the frequency response of fishes and euphausiids in the Gulf of Alaska. ICES J Mar Sci 2018;75(3):1131−42. https://doi.org/10.1093/icesjms/fsx204.
[39] Foote KG, Traynor JJ. Comparison of walleye pollock target strength estimates determined from in situ measurements and calculations based on swimbladder form. J Acoust Soc Am 1988;83(1):9−17. https://doi.org/10.1121/1.396190.
[40] Yasuma H, Sawada K, Ohshima T, Miyashita K, Aoki I. Target strength of mesopelagic lanternfishes (family Myctophidae) based on swimbladder morphology. ICES J Mar Sci 2003;60:584−91.
[41] Yamamoto N, Amakasu K, Abe K, Matsukura R, Imaizumi T, Matsuura T, et al. Volume backscattering spectra measurements of Antarctic krill using a broadband echosounder. Fish Sci 2023;89:301−15.
[42] Saygili B, Tsuyuki S, Liu J, Yamamoto N, Kobayashi K, Amakasu K. A broadband target strength measurement method for weakly scattering animals using a 50-ms-long linear frequency modulated signal in a small tank. Fish Sci 2021;87:627−38.
[43] Benoit-Bird KJ, Lawson GL. Ecological insights from pelagic habitats acquired using active acoustic techniques. Ann Rev Mar Sci 2016;8:463−90. https://doi.org/10.1146/annurev-marine-122414-034001.
[44] Jaffe JS, Roberts PLD. Estimating fish orientation from broadband, limited-angle, multiview, acoustic reflections. J Acoust Soc Am 2011;129:670−80.
[45] Kubilius R, Bergès B, Macaulay GJ. Remote acoustic sizing of tethered fish using broadband acoustics. Fish Res 2023;260:106585. https://doi.org/10.1016/j.fishres.2022.106585.
[46] Puig-Pons V, Muñoz-Benavent P, Pérez-Arjona I, Ladino A, Llorens-Escrich S, Andreu-García G, et al. Estimation of Bluefin Tuna (Thunnus thynnus) mean length in sea cages by acoustical means. Appl Acoust 2022;197:108960. https://doi.org/10.1016/j.apacoust.2022.108960.
[47] Liu J, Saygili B, Iwasa A, Yamamoto N, Imaizumi T, Amakasu K. Effects of fast Fourier transform window size on the target strength spectra of tungsten carbide spheres. Fish Sci 2023;89(2):147−57. https://doi.org/10.1007/s12562-022-01653-7.